

Research Article

Starch biopolymer films containing carbon black nanoparticles: Properties and active food packaging application

Siti Hajar Othman^{a,b,*}, Nur Syahira Zaid^a, Ruzanna Ahmad Shapi'i^b, Norhazirah Nordin^a, Rosnita A. Talib^a, Intan Syafinaz Mohamed Amin Tawakkal^a

^a Department of Process and Food Engineering, Faculty of Engineering, Universiti Putra Malaysia, 43400 Serdang, Selangor, Malaysia

^b Institute of Nanoscience and Nanotechnology, Universiti Putra Malaysia, 43400 Serdang, Selangor, Malaysia

ARTICLE INFO

Keywords:

Biopolymer
Carbon black
Film
Food packaging
Nanoparticle
Starch

ABSTRACT

Developing sustainable active food packaging films is vital to address environmental concerns and prolong the food shelf life, thereby aiding the growth of the agri-food industry. This work aims to develop active food packaging films using blends of cassava starch and different concentrations of carbon black nanoparticles (CBN; 1, 2, 3, 4 %w/v). The mechanical, thermal, barrier, UV-blocking capacity, and antibacterial characteristics of the films were characterized accordingly, and the applicability of the films as active food packaging was established on cherry tomatoes. It was found that the addition of CBN in the starch films, especially at higher concentrations, enhanced the mechanical strength, thermal stability, and water vapor permeability and oxygen transmission rate. Even with 1 %w/v loading of CBN, the films were able to block around 45 % of ultraviolet-C (UV-C) light, showing the potential to serve as sustainable UV shields that can help lengthen the food shelf life. Moreover, the addition of 2 %w/v CBN in the starch films was adequate to inhibit the *Staphylococcus aureus* and *Escherichia coli* bacteria. Cherry tomatoes packaged with films containing 2 %w/v CBN exhibited the least mold growth and the lowest percentage reduction in firmness and weight, showing the potential usage for active food packaging.

1. Introduction

Conventional food packaging materials, including polyethylene, polypropylene, and polystyrene, are predominantly derived from fossil fuels and have non-biodegradable properties. This characteristic contributes to the buildup of solid waste in landfills and oceans [1]. Nonetheless, this problem can be solved by using different materials for food packaging, including those produced from biopolymers [2]. Biopolymer materials offer a promising alternative to traditional food packaging materials because biopolymers are biodegradable, non-toxic, and widely available. These biopolymers can be categorized into two types [3]:

1. Synthetic biopolymers: e.g., polylactic acid, polybutylene succinate, and polycaprolactone
2. Natural biopolymers: e.g., starch, chitosan, cellulose, and gelatin.

Amongst the natural biopolymers, starch derived from various

botanical sources like cassava, corn, wheat, yams, and potatoes has garnered attention due to its film-forming characteristics, and starch is being explored for food packaging purposes [4]. However, starch films have poor mechanical, thermal, and barrier properties [5], but these properties can be improved by the application of nanotechnology, whereby the addition of nanosized fillers to biopolymer films will create nanocomposite films [6]. The enormous surface area reinforces the biopolymer by creating a substantial interphase or boundary area linking the fillers and biopolymer matrix, thus enhancing the properties of starch biopolymer films.

Out of the many types of nanosized fillers, recent studies have highlighted the multifunctional potential of carbon nanomaterials and justified their further exploration as fillers for food packaging materials [7]. Carbon nanomaterials generally exhibit excellent biocompatibility [8], making them suitable for contact with food products. Among carbon nanomaterials, carbon black nanoparticles (CBN) are particularly promising due to their low cost and wide industrial availability, making them suitable for large-scale production [9]. CBN has established

* Corresponding author. Department of Process and Food Engineering, Faculty of Engineering, Universiti Putra Malaysia, 43400 Serdang, Selangor, Malaysia.

E-mail addresses: s.hajar@upm.edu.my (S.H. Othman), syahirazaid6@gmail.com (N.S. Zaid), ruzannashapii91@gmail.com (R. Ahmad Shapi'i), nohaf27@gmail.com (N. Nordin), rosnita@upm.edu.my (R.A. Talib), intanamin@upm.edu.my (I.S. Mohamed Amin Tawakkal).

<https://doi.org/10.1016/j.jسامd.2025.100995>

Received 16 June 2025; Received in revised form 21 August 2025; Accepted 31 August 2025

Available online 2 September 2025

2468-2179/© 2025 Vietnam National University, Hanoi. Published by Elsevier B.V. This is an open access article under the CC BY-NC-ND license (<http://creativecommons.org/licenses/by-nc-nd/4.0/>).

applications to enhance ultraviolet (UV) resistance [10], thereby reducing UV-induced degradation of packaging materials. Similarly, carbon dots have garnered growing interest, with reports showing that their incorporation in biopolymer films can enhance tensile strength, improve barrier performance, boost UV-blocking capability, and confer antimicrobial and antioxidant effects, ultimately enhancing food preservation [11,12]. Such nanocomposites can serve as active food packaging, extending food shelf-life and maintaining food quality, with the potential to outperform conventional food packaging materials. However, the body of literature addressing carbon nanomaterials in packaging remains limited in scope, and studies specifically investigating CBN in starch biopolymer matrix are still scarce and fragmented.

Nonetheless, the attributes of nanocomposite films are influenced by the concentration of the nanosized filler incorporated in the film matrix [13]. The suitable concentration of CBN added to the starch films is an imperative parameter that is crucial to be explored because the concentration of CBN can alter the distribution or dispersion of the CBN in the nanocomposite, and affect the quality and application as an active food packaging material. Despite the promising advantages of CBN, limited work has been done to utilize it in developing food packaging material. To the best of our knowledge, no research has been conducted in relation to cassava starch/CBN films. Furthermore, there is a lack of research investigating the potential utilization of the films for active food packaging. Thus, this work aims to develop and characterize the morphological, physical, mechanical, thermal, barrier, and antibacterial attributes of starch biopolymer films incorporated with various concentrations (0, 1, 2, 3, 4 %w/v) of CBN. The application of these films as active food packaging was demonstrated on a selected food product, particularly cherry tomatoes, by evaluating the quality attributes (appearance, weight loss, and textural changes) of the cherry tomatoes packed with the produced films.

2. Materials and methods

2.1. Materials

Glycerol was bought from Sigma Aldrich (M) Sdn. Bhd., carbon black nanopowder (Purity: 99.9 %, APS: 100 nm, safe in contact with food) was purchased from Nano Life Quest Sdn. Bhd., cassava starch (food grade), calcium chloride (CaCl_2), and ethanol were bought from R&M Chemical Sdn. Bhd., sodium hydroxide (NaOH), magnesium nitrate ($\text{Mg}(\text{NO}_3)_2$), sodium bromide (NaBr), paraffin wax, and beeswax were acquired from R&M Marketing, UK. Cherry tomatoes were bought from Whole Foods Express Sdn. Bhd., Seri Kembangan, Selangor. One type of gram-positive bacteria, *Staphylococcus aureus* (*S. aureus*), and one type of gram-negative *Escherichia coli* (*E. coli*) bacteria were acquired from the Microbiology Laboratory, Faculty of Food Science and Technology, Universiti Putra Malaysia.

2.2. Preparation of films

The films were prepared via a solvent-casting method. An amount of 4 g cassava starch and different concentrations of CBN (0, 1, 2, 3, 4 %w/v) were mixed with 100 ml of distilled water. The selected concentrations of CBN were based on preliminary experiments and the findings of Das et al. [14], who recommended a maximum carbon black (CB) filler content of approximately 4 wt% because higher content tends to cause filler agglomeration, thereby compromising the tensile properties of the composite. Then, the solution was agitated for 5 min at 900 rpm using a rod on a magnetic stirrer (FAVORIT HS0707V2, Jakarta, Indonesia). Following that, 1 g of glycerol was incorporated into the solution, which was then agitated for 5 min at 900 rpm. The solutions were heated on a hotplate stirrer (Thermo Scientific Fisher (M) Sdn. Bhd., Shah Alam, Malaysia) to 80 °C and swirled for 45 min at 900 rpm. After that, the solution was cooled to 40 ± 2 °C. The solution was subsequently ultrasonicated for 10 min at 50 % amplitude using an ultrasonic probe

(QSonica, Newtown, CT, USA, 500 W, 20 kHz) to achieve a homogeneous solution. Finally, 35 ml of the solution was transferred to a Petri dish and left at room temperature (27–30 °C) until dry. The films were stored in a desiccator having $\text{Mg}(\text{NO}_3)_2$ solution (relative humidity (RH): 51 %, Temperature: 30 °C).

2.3. Characterization of films

2.3.1. Molecular interaction

The molecular interactions between CBN and the starch in the films were determined using Nicolet 6700-Thermo Nicolet, Thermo Scientific, United States. FTIR spectra for CBN were collected by employing potassium bromide (KBr) pellets at a 50:1 wt ratio of KBr:CBN. Solid-state measurements were made to obtain the FTIR spectra of the films in the wavelength range of 650–4000 cm^{-1} .

2.3.2. Physical properties

A digital micrometer (Mitutoyo, Kanagawa, Japan) was employed to determine the film thickness at five various locations of the film.

A portable colorimeter (GOYOJO, Instrument Sdn. Bhd, China) was utilized to determine the different color parameters (L^* , a^* , b^*) of the films at least at 3 different positions around the films. The total color difference (ΔE) was determined via the following equation:

$$\Delta E = [(\Delta L^*)^2 + (\Delta a^*)^2 + (\Delta b^*)^2]^{1/2} \quad (\text{Equation 1})$$

where ΔL^* , Δa^* , and Δb^* are the differential values of L^* , a^* , and b^* of neat starch and starch/CBN films, respectively.

The light transmittance percentage of the films was measured at wavelengths ranging from 200 to 800 nm. The following equation was employed to measure the opacity values of the films:

$$\text{Opacity} = (\text{T600} / 100) \times L \quad (\text{Equation 2})$$

where T600 is the value of transmittance at 600 nm and L is the film thickness (mm).

2.3.3. Morphological properties

Transmission electron microscopy (TEM; Hitachi HT7700, Japan) analysis was carried out to investigate the morphology and dispersion of CBN within the matrix of starch films. Before viewing, the films were cut using a cryo-ultramicrotome (RMC PowerTome PC, USA) to acquire a thin cross-section. After that, the cut films were attached to 300-mesh copper and examined under the TEM (magnification 10k).

2.3.4. Mechanical properties

The tensile strength (TS), elongation at break (EAB), and Young's Modulus (YM) were determined using a texture analyzer (TA.XT2 Stable Micro Systems, UK) in accordance with the American Society for Testing and Materials (ASTM) D882 [15]. The sample films were cut into 100 mm × 15 mm strips, which were then located between the grips [3]. The initial grip separation and test speed were set to 0.5 mm/s and 60 mm, respectively.

2.3.5. Thermal properties

A thermogravimetric analyzer was used to perform a thermogravimetric analysis (TGA) under a nitrogen atmosphere (Mettler Toledo, Switzerland). TGA was performed on approximately 20 mg of sample films at temperatures in the range of 25–600 °C and a heating rate of 10 °C/min. STARe Thermal Analysis Software Version 12.10 was used to analyze TGA data.

2.3.6. Barrier properties

The water vapor permeability (WVP) was measured using the modified dry cup method in compliance with Japanese Industrial Standards (JIS)-Z0208 [16]. The films were cut using a cutter into round

shapes (diameter: 7 cm) and located in a cup containing 10 g of CaCl_2 (RH = 0 %). A magnetic stirring hotplate was used to melt a combination of paraffin wax and beeswax (8:2). The wax mixture was then decanted to cover the ring of the cup, acting as a sealant. The cup was kept in a desiccator containing saturated $\text{Mg}(\text{NO}_3)_2$ to establish a steady RH of 51 % at 30 °C. The cup weight was recorded every 24 h for ten days and plotted against time. The following equation was utilized to calculate the water vapor transmission rate (WVTR):

$$\text{WVTR} = (W/t)/A \quad (\text{Equation 3})$$

where W/t is the slope of the weight change versus the time graph (g/h) and A is the transmission area of the films (28 cm²).

The following equation was used to calculate the WVP.

$$\text{WVP} = (\text{WVTR} \times L) / (P_1 - P_2) \quad (\text{Equation 4})$$

where L is the average film thickness (mm), P_1 is the water vapor partial pressure in the desiccator at RH = 51 %, 21.64×10^5 Pa, and P_2 is the water vapor partial pressure in the cup at RH = 0 %, 0 Pa.

The oxygen transmission rate (OTR) was evaluated using an oxygen permeation system fitted with a calorimetric sensor (Illinois Instruments 8501, US) according to ASTM D3985 [17]. The films (diameter: 50 cm²) were firmly sealed in the oxygen permeation system's chamber at 23 °C. The proportion of oxygen in the chamber was allowed to drop to 0 %, whereby nitrogen gas was used to wash out the oxygen. After that, oxygen gas (101.0 kPa) was allowed to flow through the film and into the chamber. The OTR was measured every 5 s, and the measurement was stopped when the OTR vs time curve reached a plateau.

2.3.7. UV-blocking capacity

The UV-blocking capacity of the films was determined by recording UV-visible spectra using a UV-1800 spectrophotometer (Shimadzu, US) in transmittance mode at a wavelength range from 0 to 550 nm. The films were held by the film holder. The instrument software was used to extract all of the data.

2.3.8. Antibacterial activity

The antibacterial activity of the films was explored via a disc diffusion assay. The gram-positive (*S. aureus*) and gram-negative (*E. coli*) bacteria were grown on nutrient agar and incubated in an incubator (Mediatech Technologies India Private Limited, India) at 37 °C. The cultured bacteria were inoculated in saline water after 24 h, and the bacterial concentration was standardized to 10^8 CFU/ml using the McFarland scale. The bacteria were then spread onto Mueller-Hinton agar in a Petri dish via the spread method. Prior to performing the antibacterial tests, the films were cut aseptically into 0.6 mm discs. The discs were carefully positioned in the Petri dish containing bacteria and incubated in the incubator for 24 h at 37 °C. The inhibition area of the film discs was observed after 24 h. F.

2.4. Demonstration of the application of the films as active food packaging materials

Cherry tomatoes were selected as the sample food product to evaluate the applicability of the films for food packaging due to their short shelf life. The cherry tomatoes were thoroughly washed using tap water and wiped using a tissue to ensure that any excess moisture was removed. Only cherry tomatoes at the matching maturity level (Stage 6: Red) were chosen [18]. They were also chosen based on uniform appearance, physical integrity, and absence of visible mold. For each replication, cherry tomatoes were sourced from the same batch to ensure consistency. The quality attributes, including physical appearance, weight loss, and texture (firmness) loss, were determined on days 0, 3, 6, 9, and 11.

2.4.1. Physical appearance

The cherry tomatoes were placed in direct contact with the films, and the transformation in the physical appearance of the cherry tomatoes was observed over time. To avoid contamination, the knife and Petri dish were first sanitized with ethanol. The films were then cut, fitting the size of the Petri dish lid, and positioned inside the lid. Following that, a cherry tomato was cut in half and placed inside the Petri dish. The Petri dish was closed using the lid, ensuring that the cherry tomato was in direct contact with the film. The sample was kept in the cold room (SNOW, Selangor, Malaysia) at 10 °C.

Transformation of the appearance of the cherry tomatoes, including mold growth, was documented by photographing the samples from the top (height: 20 cm) of the samples on days 0, 3, 6, 9, and 11 with a camera phone (iPhone 6s, Foxconn, Zhengzhou, China). The images were captured using a similar camera, lighting conditions, angle, and settings (no flash, auto mode, high dynamic range (HDR) off).

2.4.2. Weight loss and texture loss

The cherry tomatoes were packed individually in the films (dimensions: 5 cm × 7 cm) via a heat sealer. They were stored at a temperature of 10 °C in the cold room. The weight loss of the cherry tomatoes was calculated on a designated day via the following equation:

$$\text{Weight loss} = [(W_o - W_t) / W_o] \times 100 \% \quad (\text{Equation 6})$$

where W_o is the initial weight of cherry tomato (g), and W_t is the final weight of cherry tomato (g) at designated days of storage.

For texture loss, the firmness of cherry tomatoes was measured using a 2.5 mm diameter flat-tipped cylindrical probe and a 50 kg cell via a texture analyzer. The cherry tomatoes were compressed using the probe at a speed of 2 mm/s to a 2 mm penetration depth. Texture loss was determined using the following equation:

$$\text{Texture loss} = [(F_o - F_t) / F_o] \times 100 \% \quad (\text{Equation 7})$$

where F_o is the initial firmness of cherry tomato (N), and F_t is the final firmness of cherry tomato (N) at designated days of storage.

2.5. Statistical analysis

Minitab 16 (Minitab LLC, Pennsylvania, United States) software was utilized to carry out the statistical analysis of the experimental results through the application of analysis of variance (ANOVA). Mean comparisons were performed utilizing Tukey's test at a 0.05 significance level.

3. Results and discussion

3.1. Characterization of films

3.1.1. Molecular interaction

FTIR analysis was performed on the neat starch and starch/CBN (2, 4 %w/v) films to investigate the molecular interactions that occurred between CBN and starch. Fig. 1 shows the peaks at 3343 and 3344 cm⁻¹, for neat starch and starch/CBN (2, 4 %w/v) films, respectively, indicating the existence of hydroxyl groups (-OH stretching). The intensity of -OH stretching for both starch/CBN films was found to be slightly higher than the neat starch film, possibly because of the increment in hydrogen bonding in starch/CBN films. Compared to the neat starch film, the peak position of -OH stretching for starch/CBN films shifted slightly, which suggests the existence of intermolecular hydrogen bonding interactions among the hydroxyl groups of starch and hydroxyl groups of CBN. There were also C-H stretching peaks at around 2932, 2933, and 2934 cm⁻¹ for the neat starch and starch/CBN (2, 4 %w/v) films, respectively. These findings are consistent with those reported by Alaş et al. [19], who investigated the carbon dot (CD)-reinforced polyvinyl alcohol (PVA) composites for edible food packaging films. They

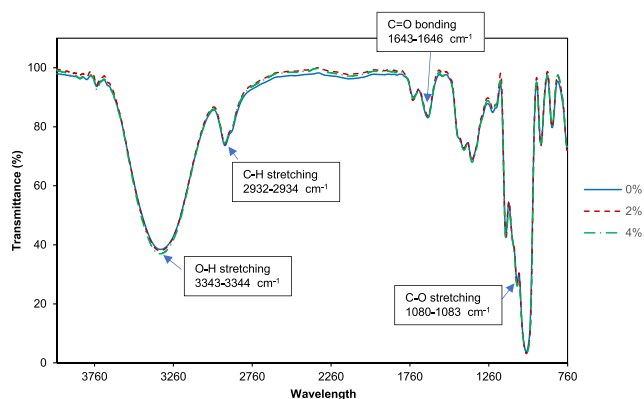


Fig. 1. FTIR spectra of the neat starch and starch/CBN (2, 4 %w/v) films.

observed a broad -OH stretching peak in the range of 3500 and 3000 cm^{-1} , attributed to intermolecular and intramolecular hydrogen bonds in PVA, and a C-H stretching peak at approximately 2905 cm^{-1} . The -OH stretching peak position of the CD/PVA nanocomposites shifted slightly, indicating the hydrogen bonding interactions between the hydroxyl groups of PVA and those on the surface of CDs.

The absorbance peaks at around 1643 to 1646 cm^{-1} and 1083 cm^{-1} for the neat starch and starch/CBN (2, 4 %w/v) films were ascribed to the hydroxyl C=O bonding and C-O stretching. No significant changes in terms of peaks were found for the starch films containing different concentrations of CBN. Overall, the neat starch film demonstrates a similar FTIR spectrum compared to the starch/CBN films, irrespective of the CBN addition and concentration, because of the similar bonds that existed in both films. These results were in line with the research of Das et al. [14], who found that the addition of carbon black into the wheat gluten polymer matrix did not alter any functional groups of the films. Alaş et al. [19] also discovered that CD inclusion in the PVA matrix did not cause the addition of new peaks or variation in the spectra because of the overlapping peaks and the small amount of CDs in the matrix.

3.1.2. Morphological properties

TEM testing was conducted to assess the dispersion of CBN within the films. Fig. 2(a) and (b) present the TEM images of starch/CBN (2 %w/v) and starch/CBN (4 %w/v) films, respectively, at a magnification of $\times 10\text{k}$. As expected, the CBN was found to be spherical in shape. As can be seen from Fig. 2, CBN was better dispersed in the starch/CBN (2 %w/v) than in the starch/CBN (4 %w/v) films. The particle sizes of CBN in starch/CBN (2 %w/v) films were in the range of 12–33 nm (Fig. 2(a)), while the particle sizes of CBN in starch/CBN (4 %w/v) films were in the range of 27–86 nm with a larger overall bulk particle size, measuring approximately 700 nm (Fig. 2(b)). Good dispersion of CBN in the films containing 2 %w/v CBN was attributed to the steric stabilization effect, which was facilitated by the starch matrix and glycerol [20] in the film formulation. It is worth mentioning that 25 %w/w of glycerol was added

to the starch/CBN films during film preparation, which was adequate to provide steric stabilization of CBN at a low loading. This observation aligns with the findings of Shapi'i et al. [3], who revealed that glycerol contributed to the steric stabilization of chitosan nanoparticles in tapioca starch film matrix, whereby starch and glycerol combined and covered the nanoparticles, generating steric repulsive forces that lead to stabilization.

Meanwhile, the poor dispersion of CBN was observed in Fig. 2(b) due to the clustering of the higher amount of CBN (4 %w/v). In this case, the starch matrix and glycerol might not create adequate bridging forces to sustain steric stabilization at higher concentrations of the nanoparticles [3]. Consequently, agglomeration of CBN within starch films occurred. This finding was consistent with the study by Koshy et al. [21], whereby they discovered that an increment in CD loading led to the agglomeration of CDs in potato starch/clitoria ternatea flower composite film. Fredi et al. [22] also found that an increment in the concentration of reduced graphene oxide in polylactide/poly(decamethylene 2,5-furandicarboxylate) composite resulted in agglomeration that led to an ineffective nanostructure in the polymer matrix, preventing the potential benefits of nanoparticles in nanocomposites from being achieved.

3.1.3. Physical properties

The thickness, color parameters (L^* , a^* , b^*), color changes (ΔE), and whiteness index (WI) of the films are tabulated in Table 1. Table 1 reveals that despite the film-forming solution volume being fixed at 35 ml, the addition of CBN slightly increased the thickness of the starch/CBN films, and the increment was prominent with the increase in CBN concentrations. The average thickness of neat starch films increased from 0.0091 to 0.1040 mm with the addition of 1 %w/v CBN, and the average thickness was further increased from 0.1040 to 0.1198 mm with the increment of CBN concentrations from 1 to 4 %w/v. This occurred because of the increase in CBN solid content, as well as the increase in the apparent size and agglomeration of CBN inside the films added with higher concentrations of CBN. Based on the studies by Albright & Hobeck [23], who investigated the physical properties of CB in spin-coated films, the agglomeration of CB observed from the microscopy images resulted in the rise of film thickness.

On the other hand, Ding et al. [24] discovered that the fish gelatin film thickness was generally increased with the addition of nano-vegetable carbon black (VCB) because fish gelatin films containing nano-VCB exhibited lower bulk densities, due to the expanded internal space of the films. In general, particle size and amount of filler added into the biopolymer matrix affected the expansion of internal space inside the films, thus the thickness. Incorporating gelatin films with equal weights of nano-VCB and larger VCB particles (3000-VCB), they revealed the nano-VCB/gelatin film to be slightly thicker, likely because the far greater number of nano-VCB particles had a stronger influence on film thickness than particle size. Hence, in this study, the thickness of starch/CBN (1, 2, 3, 4 %w/v) films increased due to the increase in the amount of added CBN. An increase in film thickness may influence several functional properties of the starch/CBN films, including opacity, mechanical, barrier, and UV-blocking properties, depending on the CBN

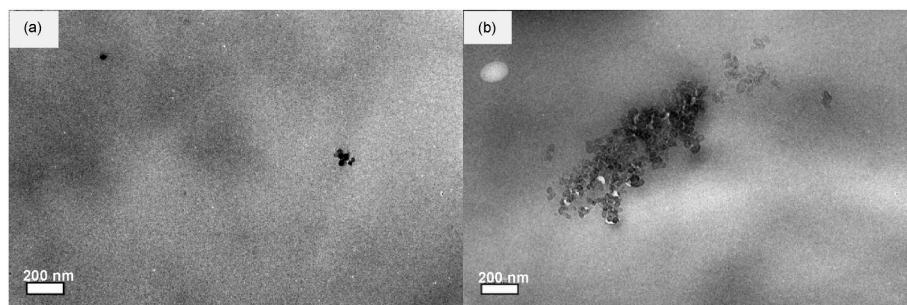


Fig. 2. TEM micrograph images of starch films incorporated with (a) 2 %w/v CBN and (b) 4 %w/v CBN at a magnification of $\times 10\text{k}$.

Table 1

Physical properties of starch/CBN films added with different concentrations of CBN. The data are reported as a mean \pm standard deviation and $p < 0.05$.

Concentration of CBN (%w/v)	Thickness (mm)	L*	a*	b*	ΔE	WI (%)
0	0.0091 \pm 0.0051 ^a	99.23 \pm 0.24 ^a	-0.26 \pm 0.04 ^a	0.74 \pm 0.61 ^a	11.42 \pm 0.24 ^a	97.97 \pm 1.32 ^a
1	0.1040 \pm 0.0047 ^{ab}	60.61 \pm 0.77 ^b	-0.46 \pm 0.07 ^b	1.34 \pm 1.07 ^b	27.31 \pm 0.78 ^a	61.02 \pm 0.61 ^b
2	0.1156 \pm 0.0067 ^{bc}	37.50 \pm 1.56 ^c	-0.71 \pm 0.03 ^c	2.20 \pm 0.16 ^c	50.41 \pm 1.56 ^b	38.22 \pm 1.08 ^c
3	0.1191 \pm 0.0064 ^{bc}	22.87 \pm 0.59 ^d	-0.84 \pm 0.04 ^d	2.91 \pm 0.20 ^c	65.05 \pm 0.59 ^c	23.66 \pm 1.20 ^d
4	0.1198 \pm 0.0060 ^c	22.03 \pm 2.63 ^d	-0.92 \pm 0.02 ^d	3.43 \pm 0.26 ^d	65.89 \pm 2.63 ^c	21.70 \pm 0.35 ^d

filler distribution and film composition. This is because thicker films tend to scatter more light, alter stress distribution during tensile testing, extend diffusion paths for gases and moisture, and increase the path length for UV absorption.

From Table 1, L* and a* values decreased while the b* values increased, and the decrement and increment were more prominent at higher amounts of CBN. This finding was consistent with the trend of results found by Campalani et al. [25], who investigated the physical properties of CDs in gelatin films. They found that as the proportion of CDs increased, there was a similar decrement pattern of L* and a* values, while there was an increment pattern in b* values, showing a greater yellow predominance in the films. Meanwhile, ΔE and WI were determined to distinguish the color changes of the films due to the incorporation of different concentrations of CBN into the starch matrix. It was found that ΔE increased, but WI decreased with the increase in concentration of CBN added to starch films. Indeed, Ding et al. [24] also found that the incorporation of nano-VCB into the gelatin films increased the ΔE values and decreased the L* and WI values due to the existence of nano-VCB, which is black in color.

Fig. 3 shows the major differences in the physical appearance of the films, which were perceived with the addition and increment of CBN in the films. The color and transparency of the neat starch film were clear and high, respectively, and the neat starch film surface was exceptionally smooth compared to the starch films containing different concentrations of CBN. The concentrations of CBN and the degrees of dispersion of the CBN inside the films affected the physical attributes of the starch/CBN films, whereby they became darker, opaque (less transparent), and rougher with the increment in the amount of CBN and agglomeration of CBN in the starch matrix (Fig. 2(b)). Ding et al. [24] also found that gelatin films became black and rough due to the dyeing properties of black pigment VCB, with nano-VCB/gelatin films appearing much

blackier and smoother than 3000-VCB/gelatin films because the smaller nano-VCB particles dispersed more effectively, enhancing light absorption and surface smoothness. In addition, agglomeration also increases the surface roughness of the films.

3.1.4. Mechanical properties

Table 2 shows that the neat starch film exhibited the lowest TS and YM; nonetheless, the highest EAB compared to starch/CBN films. The incorporation of CBN increased TS of the films, and the increment was prominent at higher CBN concentrations, whereby TS of the films increased by around 4-fold with the addition of 4 %w/v CBN, despite the agglomeration observed from TEM images (Fig. 2(b)). The presence of CBN improved the intermolecular interaction, especially through hydrogen bonds within the starch matrix as discussed in Section 3.1.1, thus bringing adjacent starch chains closer together and reducing the free volume. This led to an increase in TS. The trend observed here aligns with Das et al. [14], who reported a moderate TS increase in carbon black/wheat gluten films up to 4 wt% carbon black (4.4 MPa), with no further improvement at 6 wt% due to filler agglomeration. The higher

Table 2

(a) TS, (b) EAB, and (c) YM of the neat starch and starch/CBNs films added with different concentrations of CBN. Different letters in the same column indicate a statistically significant difference ($p < 0.05$).

Concentration of CBN (%)	Tensile strength (MPa)	Elongation at break (%)	Young's Modulus (MPa)
0	6.03 \pm 0.17 ^a	92.30 \pm 1.74 ^a	11.11 \pm 3.14 ^a
1	12.36 \pm 1.02 ^b	42.88 \pm 1.01 ^b	55.50 \pm 37.70 ^b
2	13.78 \pm 0.60 ^b	35.01 \pm 6.14 ^b	86.44 \pm 1.22 ^b
3	15.39 \pm 0.85 ^c	13.23 \pm 3.03 ^c	148.00 \pm 42.20 ^c
4	24.38 \pm 1.19 ^d	5.13 \pm 1.46 ^c	189.40 \pm 0.85 ^c

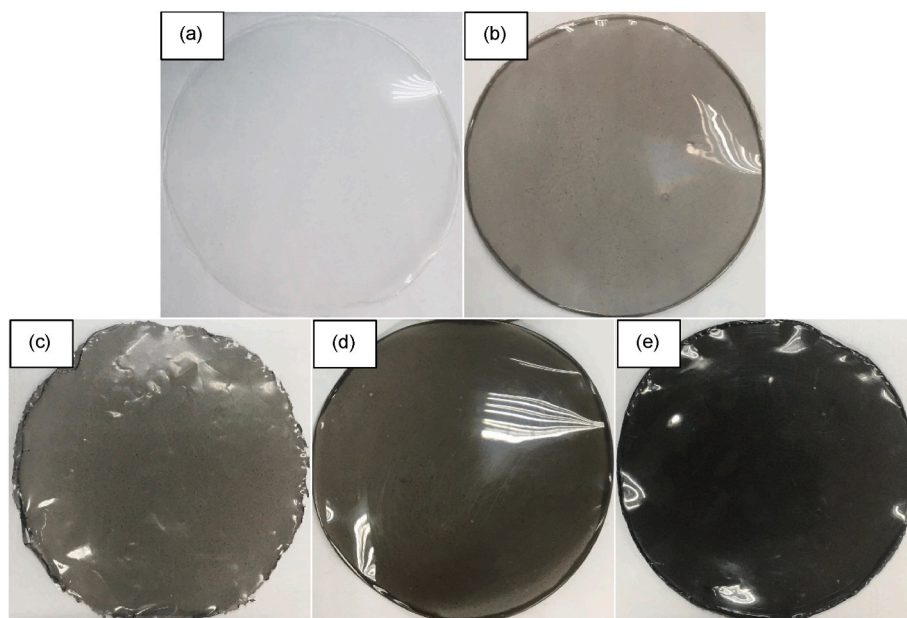


Fig. 3. Appearance of the (a) neat starch, (b) starch/CBN (1 %w/v), (c) starch/CBN (2 %w/v), (d) starch/CBN (3 %w/v), and (e) starch/CBN (4 %w/v) films.

TS values in this work are likely attributed to differences in biopolymer type, carbon black characteristics, and filler concentration. The TS of starch/CBN films revealed in this work was in the range of 12.36–24.38 MPa, which was acceptable for application, providing sufficient strength for handling and packaging operations, since the TS range was within the range of the common food plastics, particularly low-density polyethylene (LDPE; 8.3–31.4 MPa) [26].

Table 2 also reveals that CBN inclusion reduced the EAB compared to neat starch films, and the decrement became prominent at higher concentrations of CBN. EAB decreased by about 18-fold with the addition of 4 %w/v CBN. At higher CBN concentrations, CBN particles filled in the empty spaces within the starch matrix, resulting in the formation of strong hydrogen bonds as discussed in Section 3.1.1. This increased bonding strength led to the observed increase in TS and decrease in EAB of the films. The findings on EAB are consistent with Ding et al. [24], who attributed the reduced EAB of nano-VCB/gelatin films to the rigid filler limiting chain mobility and film uniformity, resulting in less ductile and deformation-resistant films. Nevertheless, the EAB values obtained in this work were not comparable to those of common plastic food packaging, particularly LDPE, but from the observation, the films could still be used to package food, as demonstrated in Sections 2.4.2 and 3.2.2.

Table 2 also shows the increment in YM with the rise of the concentration of CBN. The addition of 4 %w/v CBN increased YM by about 17-fold from 11.1 to 189.4 MPa. This increment was expected since TS increased and EAB declined when the concentration of CBN increased. Likewise, Campalani et al. [25] found that YM increased from 160 to 185 MPa as the concentration of the CDs was increased from 0 to 3 % w/v due to the reinforcing effect of CDs in the gelatin films. In this study, the YM of neat starch film was the lowest and fell outside the range of LDPE films [26]. Nonetheless, starch/CBN (4 %w/v) films had an average YM value of 189.40 MPa, which fell in the YM range of LDPE films (172–282 MPa).

It is worth noting that although the TS and YM of the films increased with the increase in CBN concentrations, the EAB decreased, indicating reduced flexibility. Undeniably, a decrease in EAB can limit the suitability of the films for flexible packaging applications. Nonetheless, films containing 2 %w/v CBN strike an optimal balance between strength and flexibility, making them suitable for applications that require moderate mechanical performance. The measured TS (13.78 MPa) and YM (86.44 MPa) ensure sufficient mechanical integrity for handling and maintaining package shape, while moderate EAB (35.01 %) provides enough flexibility to wrap around irregular produce surfaces without cracking, as demonstrated in Sections 2.4.2 and 3.2.2.

3.1.5. Thermal properties

Fig. 4 demonstrates that the degradation process observed in the neat starch and starch/CBN films occurred at two distinct sequential stages. The first stage occurred between 50 and 150 °C, which was commonly

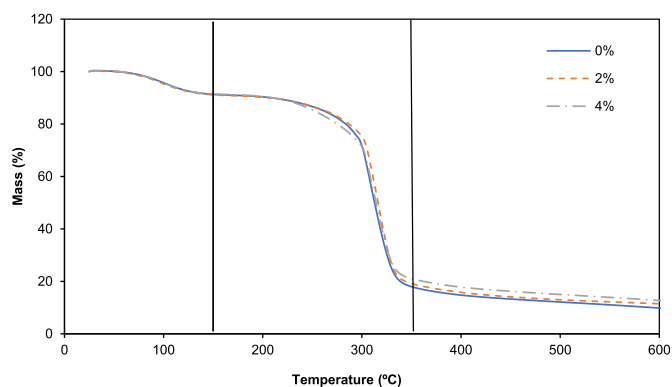


Fig. 4. Thermal analysis of the neat starch and starch/CBN (2, 4 %w/v) films.

attributed to weight loss due to moisture loss. The second stage, starting at around 150 °C and concluding at around 330 °C, was commonly associated with the breakdown of glycerol and starch chains. On the other hand, carbon black requires a higher temperature than 500 °C to degrade [27]. These findings are consistent with the results of Campalani et al. [25], who also observed that the temperatures for the first and second stages of thermal decomposition of gelatin films containing CDs were in the ranges of 45–110 °C and 125–325 °C, respectively. The specific TGA parameters, including onset temperature (Tonset), temperature at maximum degradation (Tmax), and residual ash weight (%) for the second stage of thermal decomposition, were compiled and presented in Table 3.

Table 3 shows that the Tonset of starch films rose from 158.37 to 160.39 °C with the inclusion of 2 %w/v CBN implying that the inclusion of CBN raised the energy requirement (higher Tonset) for the films to initiate degradation due to the molecular interaction through hydrogen bonds between CBN and starch matrix as proven from FTIR results (Section 3.1.1). The Tonset further increased to 169.41 °C when a higher concentration of 4 %w/v CBN was incorporated. Venkatesan et al. [28] reported that incorporating carbon nanoparticles into poly(butylene adipate-co-terephthalate) (PBAT) biopolymer improved thermal stability and resistance to high temperatures, particularly at higher concentrations, due to their ability to graft onto polymer chains and enhanced compatibility, dispersion, and overall matrix interactions.

Table 3 also shows that Tmax increased from 308.47 to 317.06 °C when 2 %w/v CBN was included in the starch matrix, indicating enhancement in the thermal stability of films that require high energy to degrade. Nonetheless, when the concentration of CBN in the starch matrix was increased to 4 %w/v, Tmax decreased slightly from 317.06 to 313.48 °C, probably attributed to the agglomeration as was seen from the TEM image of starch/CBN (4 %w/v) film (Fig. 2(b)). CBN tends to agglomerate as its concentration rises, which develops structural flaws in the matrix. Consequently, the thermal stability of the films was slightly compromised, leading to degradation at a lower temperature. The presence of agglomerated CBN particles reduced the energy required for complete degradation, contributing to lower thermal stability. These findings align with the mechanical analysis result (Section 3.1.4), where the EAB of starch/CBN (4 %w/v) was low (5.13 %) and the TS was high (24.3 MPa), indicating that the film was likely brittle, thus reducing the energy required to degrade. Nonetheless, Tmax for starch/CBN (4 %w/v) films was still higher than neat starch films, demonstrating the advantage of adding CBN despite the agglomeration.

Meanwhile, the ash residual of starch/CBN (2, 4 %w/v) films was higher than neat starch film due to the existence of carbon nanoparticles, which had higher crystallinity [29] and a more compact structure, making it more challenging to break down than starch, which had a greater amorphous content. Apart from that, carbon black also requires a high temperature to decompose [27]. The ash residual for starch/CBN (4 %w/v) film was slightly higher than starch/CBN (2 %w/v) film due to the higher amount of CBN in the starch/CBN (4 %w/v) film. Moreover, the addition of CBN in the films also prevented volatile substances trapped in the starch matrix from diffusing, thus delaying the decomposition process of starch films, resulting in higher ash residue. Mousa et al. [30] found that the increment in the concentration of carbon bamboo nanoparticles delayed the thermal degradation of PVA because carbon bamboo nanoparticles acted as material barriers that hindered volatile degradation products. In addition, Venkatesan et al. [28] also

Table 3

TGA parameters for neat starch and starch/CBN films at the second stage of thermal decomposition.

Sample film	Tonset (°C)	Tmax (°C)	Ash residual (%)
Neat starch	158.37	308.47	9.82
Starch/CBN (2 %w/v)	160.39	317.06	11.46
Starch/CBN (4 %w/v)	169.41	313.48	12.68

indicated that carbon nanoparticles have the ability to act as a barrier that limits biopolymer diffusion as well as oxidative degradation, thus contributing to an increase in thermal stability.

3.1.6. Barrier properties

Fig. 5 demonstrates the effects of CBN inclusion on the WVP and OP of starch films. The inclusion of CBN from 1 to 3 %w/v into starch films was found to slightly increase the WVP, but the increment was prominent at 4 %w/v CBN (Fig. 5(a)). Consistent with the trend of WVP, the inclusion of CBN in the starch film also raised OTR, and the increment became predominant at higher concentrations of CBN (Fig. 5(b)). This was due to the high CBN concentration that resulted in larger agglomerates of CBN, as can be observed from the TEM figure (Fig. 2(b)). The agglomeration between starch and CBN provoked the pathways or channels for moisture and oxygen gas to permeate the films, hence increasing the WVP and OTR.

Beyond agglomeration, several factors may contribute to the reduced barrier performance observed with increasing CBN content. The poor interfacial adhesion between the hydrophobic CBN and the hydrophilic starch matrix could result in microvoids or weak interfacial zones that facilitate gas and vapor permeation [31,32]. Additionally, the incorporation of rigid CBN particles may disrupt the continuity of the starch polymer network, creating preferential diffusion pathways that compromise barrier integrity [33]. Although Section 3.1.4 highlights improved intermolecular interactions via hydrogen bonding contributing to enhanced TS by reducing free volume, this structural improvement may not have directly translated into improved barrier properties. The tortuous path mechanism is typically associated with nanosized fillers that rely heavily on uniform dispersion and strategic alignment, conditions which may not be fully realized in this system [34]. Furthermore, increased surface roughness at higher CBN

concentrations could promote localized moisture accumulation and facilitate permeation through capillary-like pathways on the film surface [35].

The WVP trend observed here is consistent with Kwaśniewska et al. [36], who reported that increased powdered activated carbon (PAC) filler content up to 15 wt% in starch films resulted in an increase in WVP due to macroscopic separation or aggregation in the films, creating diffusion pathways within the matrix. Jin et al. [37] found that increasing graphene content beyond 0.1 wt% in graphene/nylon nanocomposites led to higher WVP and OTR due to interfacial pathways formed by graphene aggregation at higher loadings. This occurrence, often called 'percolation,' happens when channels created by interfacial regions allow water to move through the polymer film more easily [38]. Hence, a high agglomeration of CBN in starch caused the pathways or channels for moisture or gases to absorb and permeate the films.

The films incorporated with 2 %w/v CBN exhibited a moderate WVP value (31.05 g/m²·day after conversion), which is competitive relative to other biodegradable polymers, which typically exhibit WVP values in the range of 13 to 2900 g/m²·day [39]. Although higher than the WVP of conventional LDPE at approximately 1 g/m²·day under standard conditions [40], this WVP level is advantageous in applications such as fresh produce packaging, where a certain degree of moisture transmission is required to prevent excessive condensation while slowing respiration-driven moisture loss and deterioration. In terms of oxygen transport, the films demonstrated a high OTR (14,577.5 cm³/m²·day), which places them in the low-barrier category [41]. While this relatively high OTR makes the films unsuitable for highly oxygen-sensitive foods such as meat or dairy, it can be advantageous for packaging fresh fruits and vegetables, where controlled oxygen permeability helps maintain aerobic respiration and delays the onset of anaerobic spoilage.

3.1.7. UV-blocking capacity

Table 4 tabulates the percentage transmittance of the films at different UV spectrums (wavelength: 365 nm - UV-A; 300 nm - UV-B; 275 nm - UV-C) and visible light (wavelength: 550 nm), as well as the opacity. The transmittance of the films under all regions declined with the addition and rise in the loading of CBN in starch films. The decrease in transmittance indicates a decrease in the transparency of films. For the visible light, the transmittance dropped from 79.0 to 30.6 % with the addition of 4 %w/v CBN. The percentage transmittance of starch/CBN films was also reduced at the different UV spectrums (275–365 nm) with the increment in the amount of CBN, revealing an increase in UV-blocking capacity. Higher CBN concentration resulted in a higher UV-shielding behavior of the films, reaching a capacity to block nearly 80 % of the UV-C light (starch/CBN 4 %w/v) due to the UV absorption ability of the CBN. Sharif Sh. et al. [42] investigated the dispersion and stability of CBN using UV-visible spectroscopy and attributed an improvement of UV absorption to the increase in the total CBN area exposed to UV light, which led to the increment of the number of π - π^* excitations. UV absorption in carbon materials is associated with the electronic transitions between the bonding and anti-bonding of π orbital [43], whereby an increase in π - π^* excitations can improve UV absorption. Therefore, a greater UV-vis absorption might be anticipated by enhancing the amount and dispersion quality of CBN in the film matrix.

The pattern of the result is aligned with the work of Campalani et al. [25], who found that as the concentration of CDs in gelatin films increased, the value of transmittance of the UV light decreased, achieving the capability of blocking around 70 % of UV. With the capacity to block UV, the starch/CBN films could be applied for UV-sensitive food packaging applications such as vitamins and dairy products since UV can damage food often due to auto-oxidation, which is directly induced by energy input from light [44,45].

Meanwhile, Table 4 also shows that the opacity of films somewhat rose with the inclusion and with the increase in the concentration of CBN, implying a decrease in the transparency, in line with the percentage transmittance results. The opacity of starch films increased from

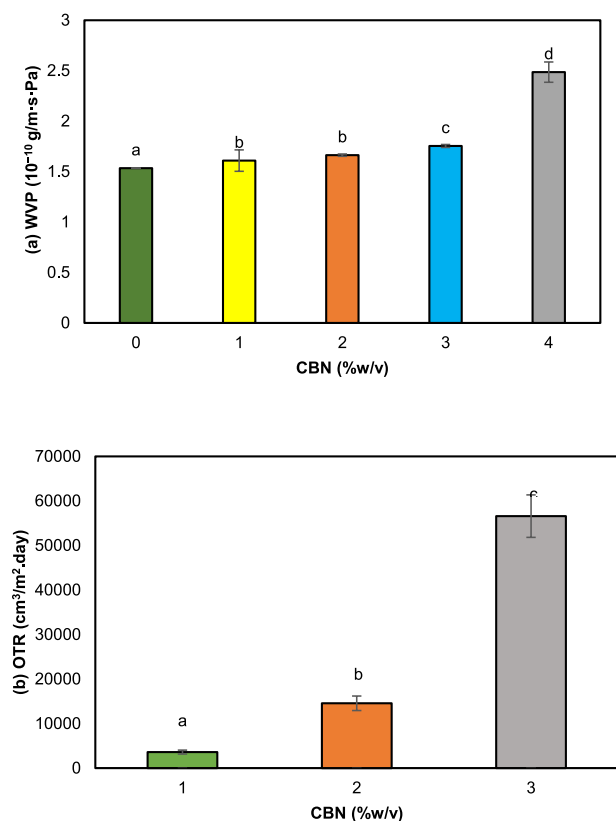


Fig. 5. Effect of CBN concentration on (a) WVP and (b) OP of starch films. The data are reported as a mean \pm standard deviation. Different letters indicate a significant difference at $p < 0.05$.

Table 4

The transmittance (%) of the neat starch and starch/CBN (1, 2, 3, 4 %w/v) films at different UV spectrums and visible light, as well as the opacity of the films. Different letters in the same column indicate a statistically significant difference ($p < 0.05$).

Concentration (%)	Transmittance (%)				Opacity (nm/mm)
	275 nm (UV-C)	300 nm (UV-B)	365 nm (UV-A)	550 nm (Visible Light)	
0	61.3 \pm 1.6 ^a	66.8 \pm 1.7 ^a	71.6 \pm 1.8 ^a	79.0 \pm 1.5 ^a	1.28 \pm 0.14 ^a
1	44.8 \pm 4.3 ^b	49.5 \pm 3.4 ^b	52.5 \pm 3.7 ^b	51.1 \pm 2.9 ^b	2.46 \pm 0.33 ^b
2	35.9 \pm 1.9 ^c	37.8 \pm 1.2 ^c	40.8 \pm 1.1 ^c	44.0 \pm 1.5 ^c	3.49 \pm 0.36 ^{bc}
3	31.9 \pm 2.8 ^c	34.0 \pm 2.9 ^c	36.9 \pm 2.6 ^c	43.0 \pm 2.7 ^c	4.08 \pm 0.03 ^c
4	19.3 \pm 1.5 ^d	20.6 \pm 1.5 ^d	22.6 \pm 1.5 ^d	30.6 \pm 1.5 ^d	5.54 \pm 0.46 ^d

1.28 to 5.54 (nm/mm) with the inclusion of 4 %w/v CBN. This finding was in agreement with the findings by Kavooosi et al. [46], whereby the opacity of the gelatin film containing multi-walled carbon nanotube (MWCNT) increased with the increase in the concentration of MWCNT from 0.5 to 2 %w/v. This can be associated with the nanosized fillers that do not dissolve in the matrix, hence decreasing the film transparency, and leading to a higher opacity [47]. As a result, the starch films ceased to have their usual colorless and translucent aspect with the addition of CBN. However, despite the reduction in opacity, the resulting starch/CBN films exhibited UV light barrier properties that are useful in preventing UV-induced lipid peroxidation in certain food applications [48]. The UV-blocking capability mitigates photooxidation and light-induced degradation of nutrients and pigments, a critical factor for light-sensitive foods.

3.1.8. Antibacterial activity

Fig. 6(a) and (b) present the images of the inhibitory zone of gram-positive and gram-negative bacteria that are *S. aureus* and *E. coli*, respectively, for neat starch and starch/CBN films. For neat starch films, no bacterial inhibition zone was seen for both bacteria due to the non-existence of CBN, which exhibits antimicrobial activity [49]. Nonetheless, there was a slightly clear inhibition zone of bacteria for starch/CBN (1 %w/v) films, but the concentration of 1 %w/v CBN might be low and not enough to inhibit the bacteria from growing under the films. Clear inhibition zones can only be observed for *E. coli* and *S. aureus* bacteria under the starch/CBN (2 %w/v) films, demonstrating that at least 2 % w/v CBN was required to inhibit both the *E. coli* and *S. aureus* bacteria. Furthermore, Fig. 6 also reveals that the inhibitory zones of both bacteria for starch/CBN (2, 3, 4 %w/v) films only occurred under the films where they were in direct contact with the films. This was because CBN is not volatile and thus could not diffuse to inhibit the bacteria not in direct contact with the films. Nevertheless, the demonstrated antibacterial activity of the films incorporated with CBN against *S. aureus* and *E. coli* demonstrated that the films have the potential to reduce microbial

spoilage and contamination risks of food, providing an active protection layer that extends food shelf life.

The findings of this study align with Fan et al. [50], who revealed that increasing CD concentration (0–4.5 %) in chitosan films increased antibacterial activity. On the other hand, Li et al. [51] found that CDs exhibited strong antibacterial activity against *E. coli* and *S. aureus* at 1000 μ g/mL, with SEM images revealing bacterial cell wall damage and cytoplasmic leakage as the main mechanism. They also observed that increasing CD loading altered the deoxyribonucleic acid (DNA) circular dichroism spectrum, indicating disruption of DNA secondary structure. The unwinding process of DNA by CDs had also been predicted using simulations [52]. The secondary structure of DNA is disrupted when terminal base pairs interact with CDs.

Although an antibacterial mechanism study of CBN was not conducted in this work, previous literature suggests that CBN may exhibit potent antibacterial activity through multiple synergistic mechanisms. One possible primary mode involves direct physical interaction with bacterial membranes, where the hydrophobic surface chemistry of CBN promotes adhesion to the lipid bilayer, and the nanoscale surface roughness exerts mechanical stress that compromises membrane integrity, leading to increased permeability and leakage of intracellular contents [53]. Additionally, CBN may catalyze the generation of reactive oxygen species (ROS), such as superoxide anions and hydroxyl radicals, which induce oxidative stress and damage essential biomolecules, including proteins, lipids, and DNA [54]. The high surface area of CBN may also enable the adsorption of vital nutrients and signaling molecules from the bacterial microenvironment, effectively starving cells and disrupting metabolic functions [55]. Under light exposure, CBN may further contribute to bacterial inactivation via photothermal effects, where absorbed light energy is converted into localized heat, enhancing antimicrobial efficacy [56].

In the current study, the dispersion of CBN within the starch matrix is facilitated by hydrogen bonding and van der Waals interactions between the hydroxyl groups of starch and the surface functionalities of CBN.

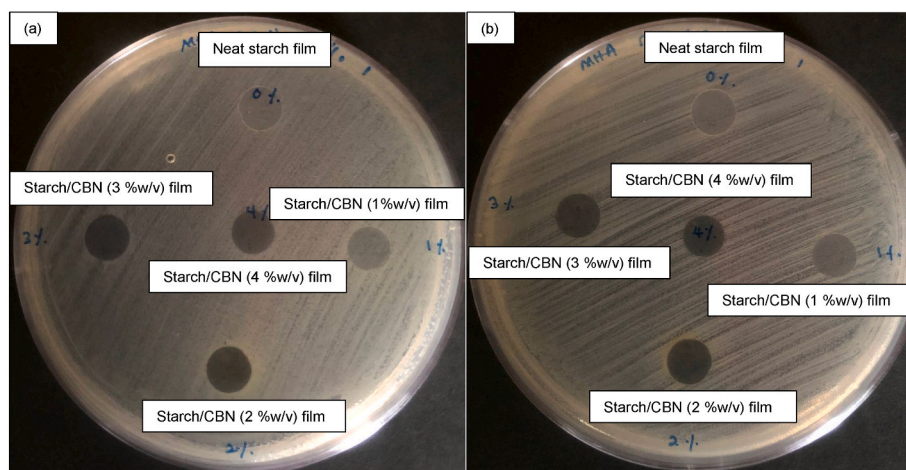


Fig. 6. Inhibitory zones of neat starch films and starch/CBN films for (a) *E. coli* and (b) *S. aureus*.

This interaction may influence the molecular mobility and crystallinity of starch biopolymer, potentially affecting the diffusion and the accessibility of CBN to microbial cells. The non-volatility and contact-dependent nature of CBN explain the limited antibacterial performance observed in disc diffusion assays, where no significant inhibition zones were detected across the tested concentrations of CBN. This suggests that the antibacterial efficacy of CBN is likely localized at the film-bacteria interface rather than diffusive. Additional mechanistic studies, including surface characterization and microbial adhesion assays, are warranted to elucidate the role of CBN in antibacterial performance.

3.1.9. Benchmarking against literature

To provide context for the functional performance of starch/CBN films, a comparative analysis with carbon-based biocomposite films reported in the literature is presented in Table 5. The comparison covers mechanical, thermal, barrier, UV transmittance, and antibacterial properties. Results show that starch/CBN films achieve a balanced combination of tensile, thermal, water vapor permeability, and antibacterial properties, along with enhanced UV protection, demonstrating their competitiveness with other films and confirming their potential for active food packaging applications.

Table 5

Comparative properties of starch/CBN films (this work) and other carbon-based biocomposite films reported in the literature, including mechanical, thermal, barrier, UV transmittance, and antibacterial performance.

Matrix + Filler	Filler Concentration	Mechanical Properties	Thermal Properties	Barrier Properties	UV Transmittance	Antibacterial	Reference
Cassava starch + CBN (this work)	0, 1, 2, 3, 4 % w/v	TS: 6.03–24.08 MPa EAB: 5.13–92.3 % YM: 11.11–189.40 MPa	Tonset: 158.37–169.41 °C Tmax: 308.47–313.48 °C Ash residual: 9.82–12.68 % No ratings in vertical burn tests	WVP: 1.534×10^{-10} -2.486 $\times 10^{-10}$ g/m ² ·s·Pa OTR: 3602.9–56580.9 cm ³ /m ² ·day	UV-C: 19.3–61.3 % UV-B: 20.6–66.8 % UV-A: 22.6–71.6 %	Inhibitory zones under starch/CBN (2, 3, 4 % w/v) films against <i>E. coli</i> , <i>S. aureus</i>	This study
Wheat gluten + CBN	0, 2, 4, 6 wt%	TS: ~3–4.5 MPa EAB: ~0.1–1.25 mm/mm YM: ~50–225 MPa Energy at break: ~0.1–1 J	N/A	Water sorption (WS): 26.91–41.51 % increase	N/A	N/A	[14]
Fish gelatin + nano-VCB	20 %v/v	TS: 52.589 MPa EAB: 8.912 % YM: 968.874 MPa	N/A	WVP: $\sim 1.75 \times 10^{-11}$ g/m s Pa OTR: 1.510 cm ³ /m ² ·day	200–400 nm: ~15 %	N/A	[25]
PVA + CDs	0, 0.25, 0.5, 1.0, 2.0 wt%	N/A	Temperature at 50 % weight loss: 322.5–347.3 °C Weight loss at Tmax: 100–95.86 % Residue at 800 °C: 0–4.14 %	N/A	UV-C: 7.78–76.86 % UV-B: 12.96–75.68 % UV-A: 23.23–79.25 %	Minimum inhibitory concentration (mg/L) <i>E. coli</i> : 128–256 <i>B. cereus</i> : 64–256 <i>S. aureus</i> : 256 <i>E. hirae</i> : 64–128 <i>P. aeruginosa</i> : 18–64 <i>L. pneumophila</i> sbsp. <i>pneumophila</i> : 64–128	[19]
Gelatin + CDs	0, 1, 3, 5 %w/w	TS: 12–10 MPa EAB: 27–40 % YM: 80–185 MPa	Glass transition temperature: ~25–50 °C, independent of CDs content	WS: 54.9–70.1 % WVP: 0.75×10^{-7} – 1.05×10^{-7} g/h m Pa	UV-C: 28.9–60.6 % UV-B: 50.7–81.9 % UV-C: 70.6–86.4 %	N/A	[26]
Starch + PAC	1–5, 10, 15 wt %	TS: 1.86–3.42 MPa Maximum strain: 0.16–0.53 YM: 17.95–79.65 MPa	N/A	Water solubility index: 30.54–32.14 % WVP: 2.60×10^{-10} – 4.13×10^{-10} g/m s Pa	N/A	N/A	[32]
Nylon + graphene	0.1, 0.3, 0.6, 1, 3 wt%	Yield strength: 37.9–45.4 MPa Stress at break: 21.0–55.9 MPa EAB: 3.7–321.72 MPa YM: 900–1510 MPa	Crystallization temperature: 155.2–167.8 °C Melting temperature: 180.8–194.7 °C	WVP: 15.7–36.3 g ml/m ² ·day OTR: 10.1–27.6 cm ³ /m ² ·day	N/A	N/A	[33]
Chitosan + CDs	0, 1.5, 3, 4.5 % v/v	N/A	N/A	N/A	N/A	Inhibition zone diameters (mm) <i>S. aureus</i> : 9.10–13.01 <i>E. coli</i> : 9.32–12.77	[43]

3.2. Demonstration of the application of the films as active food packaging materials

Cherry tomatoes were packaged in the developed films, and the attributes of cherry tomatoes were assessed in regard to physical appearance, weight loss, and firmness loss.





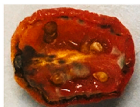




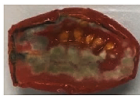




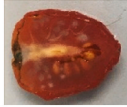















3.2.1. Physical appearance

The mold growth on cherry tomatoes was visually observed over storage at 10 °C from day 0 to day 11th as tabulated in Table 6. It was discovered that mold grew more slowly on cherry tomatoes in direct contact with starch/CBN films compared to control cherry tomatoes (no packaging films) and cherry tomatoes in direct contact with neat starch films. This occurred because of the presence of CBN, which exhibits antibacterial activity as discussed in Section 3.1.8.

The mold on cherry tomatoes started to grow on day 9, and the most obvious mold growth can be seen on control cherry tomatoes, followed by cherry tomatoes in direct contact with neat starch and starch/CBN (4 %w/v) films. Mold growth was not detected for cherry tomatoes in direct contact with starch/CBN (1, 2, 3 %w/v) films on day 9. After the 11th day, cherry tomatoes in direct contact with neat starch films had the most mold, probably because of the lowest WVP and OP values (Fig. 5), which disturbed the respiration process of cherry tomatoes.

Table 6

Appearance of sliced cherry tomatoes, including control (no packaging films) and in direct contact with the neat starch and starch/CBN (1, 2, 3, 4 %w/v) films.

Concentration (%)	Storage Time (Day)				
	0 th	3rd	6th	9th	11th
Control					
0					
1					
2					
3					
4					

Respiration is a vital metabolic process in fruits, where fruits take in oxygen and release water vapor and carbon dioxide. The rate of respiration can affect the ripening, shelf life, and overall traits of fruits [57]. If the packaging film restricts oxygen entry, it can create an anaerobic environment inside the package, leading to anaerobic respiration, resulting in the production of undesirable metabolic byproducts like ethanol and off-flavors, leading to fruit decay and poor quality [58]. Nonetheless, it is worth noting that packaging film that allows too much oxygen to enter the package can lead to increased respiration in the fruits. This can also hasten the ripening process, resulting in early spoilage and shorter shelf life [59]. This is particularly undesirable for fruits that have a short shelf life, such as cherry tomatoes.

On the other hand, if the packaging film restricts water vapor transmission too much, it can create a high-humidity environment within the package, which leads to increased microbial growth, mold formation, and decay of the fruits [60]. It is also worth noting that if packaging film allows excessive water vapor transmission, it can lead to moisture loss from the fruits, resulting in dehydration, shriveling, and reduced fruit weight. It can also lead to a higher concentration of sugars and acids, affecting the flavor profile and altering the fruit's sensory attributes [61]. Thus, it is essential to optimize the WVP and OP of packaging films by balancing between providing enough oxygen for normal respiration and allowing controlled water vapor transmission to maintain an optimal level of humidity. Different fruits have different respiration rates and sensitivity to these factors; thus, the packaging requirements will differ based on the specific fruit type being packaged.

Among the different starch/CBN films, starch/CBN (4 %w/v) films exhibited the poorest ability to reduce mold growth. As discussed before, the WVP and OP of starch/CBN (4 %w/v) films were the highest (Fig. 6), thus more water vapor and oxygen can diffuse, creating a favorable environment for mold growth, whereby moisture and oxygen are the

source for mold to thrive [62]. Table 6 also demonstrates that starch/CBN (2 %w/v) film was the optimal packaging film that can maintain the cherry tomatoes' shelf life throughout the 11th day, during which the sliced cherry tomatoes' appearance was still red in color and exhibited the least shrinkage after the 11th day of storage. No mold growth was also observed, which indicated a better quality of cherry tomatoes. This was due to the antimicrobial activity of the good-dispersed CBN (Fig. 2) as well as the optimal WVP and OP values (Fig. 5) of the films. The findings of this work agree with Alaş et al. [19], who showed that CD/PVA-coated strawberries stored at 4 °C remained mold-free, hydrated, and red in color for 12 days, unlike PVA-coated and uncoated strawberries that spoiled with mold after 6 days.

3.2.2. Weight loss and textural changes

Fig. 7(a) and (b) display the weight loss and firmness loss of unpackaged and packaged cherry tomatoes with the developed films stored for 11 days and kept at 10 °C. Weight loss of fruit throughout storage primarily happens due to water loss because of the transpiration process [63]. Weight loss of fruit can also occur due to damage to the fruit [64]. Fig. 7(a) demonstrates that the weight loss (%) of all cherry tomatoes was proportional to the number of storage days. The weight loss of cherry tomatoes packaged with films containing various concentrations of CBN (1, 2, 3, 4 %w/v) on the 11th day of storage was lower than that of the control and the neat starch film. It was expected that control cherry tomatoes would exhibit the most weight loss because of the absence of a barrier around the fruit. Meanwhile, cherry tomatoes packaged in the neat starch film exhibited higher weight loss than that of starch/CBN films, although the WVP of starch/CBN films was slightly higher than the WVP of the neat starch film (Fig. 5(a)). It can be hypothesized that the slight differences in WVP might not affect the moisture loss of cherry tomatoes, hence the weight loss. The weight loss

of cherry tomatoes in this study was mainly due to the microbial action that caused damage to the cherry tomatoes.

Furthermore, the weight loss of cherry tomatoes packaged with starch/CBN (1 %w/v) films was the lowest on the 11th day of storage, followed by starch/CBN (2, 3, 4 %w/v) films, following the trend of the WVP and OP values as discussed in Section 3.1.6. The higher WVP and OP of films escalated the humid condition and oxygen amount in the package, favoring the mold and bacteria growth, which damaged the cherry tomatoes and increased the weight loss. The pattern of these findings was consistent with Venkatesan et al. [28], who reported that carrots wrapped with PBAT/tannic acid/carbon nanoparticle films exhibited lower weight loss than those wrapped with PBAT neat film and control carrots, attributed to the synergistic effect of biocompatible constituent in tannic acid, the reactive moiety in PBAT, and carbon nanoparticles. Fan et al. [50] also found that incorporating CDs into chitosan films reduced the weight loss of fresh cucumber. However, instead of due to the fruit damage, they attributed this to the many functional groups in the chitosan solution that increased the degree of surface crystallization of the CD/chitosan coating, creating strong barriers against water vapor permeability.

In terms of firmness, Fig. 7(b) shows that the firmness loss (%) of all cherry tomatoes was proportional to the time of storage, whereby firmness loss increased with the increase in time of storage because of the softening process experienced by the fruit or vegetable over time [50]. The control cherry tomatoes stored without any packaging exhibited the maximum percentage loss in firmness throughout the storage, which was 27.6 %, followed by cherry tomatoes packaged in neat starch films (27.0 %). The reduction in cherry tomatoes packaged with the starch/CBN films was lower compared to the control cherry tomatoes and cherry tomatoes packed in neat starch films because of the existence of CBN that acted as an antimicrobial agent [13], which inhibited the microbial action contributing to the firmness loss [65]. Fan

et al. [50] found that CDs in chitosan films reduced the loss of firmness of fresh cucumbers due to a decrease in oxygen and water availability and thus, a decrease in metabolic rate. However, in this study, OP and WVP of starch/CBN films were higher than neat starch films; thus, it can be speculated that the microbial action causing cherry tomato injury was the dominant factor that contributed to the firmness loss of cherry tomatoes than WVP and OP of the films.

Despite the cherry tomatoes packaged in starch/CBN (1, 2, 3, 4 %w/v) films being better than the control and neat starch films in terms of firmness, however, when compared among the starch/CBN films, the percentage of firmness loss rose with the rise in the concentration of CBN. This finding can be explained by the WVP and OP results, whereby as the concentration of CBN augmented, the WVP and OP also augmented. The higher permeability allowed for easier moisture loss and oxygen gas permeation through the films, creating pathways or channels for these substances to damage the cherry tomatoes [36]. Among the starch/CBN films, the cherry tomatoes in starch/CBN (4 % w/v) film exhibited the highest weight and firmness loss compared to starch films with lower concentrations of CBN (1, 2, 3 %w/v).

4. Conclusion

The starch/CBN films were successfully developed for possible use in active food packaging. The inclusion of CBN in the starch films altered the transparency and color properties, particularly at higher CBN concentrations. The TS, YM, and thermal stability of films improved because of the strong intermolecular interactions, especially via hydrogen bonding between starch and CBN. However, CBN at higher concentrations led to agglomeration, which reduced the barrier properties of the films. The starch/CBN films also demonstrated good UV-blocking capability. Incorporating 2 %w/v CBN was sufficient to prevent bacterial growth, particularly *E. coli* and *S. aureus*. Cherry tomatoes packaged with the starch/CBN films showed less mold growth, firmness loss, and weight loss compared to both the control and neat starch films.

The optimal concentration of CBN that provides the best performance was found to be 2 %w/v. At this concentration, the films exhibited good CBN dispersion, improvement in mechanical and thermal properties, moderate WVP and OP, enhanced UV blocking capacity, and sufficient antibacterial activity. This concentration also resulted in the best preservation performance for cherry tomatoes, reducing both weight and firmness losses. Overall, the starch/CBN films developed in this study demonstrate strong potential as sustainable active food packaging, contributing to preservation and shelf life extension of food. This work is the first to report cassava starch films reinforced with CBN for active food packaging, combining environmental sustainability with demonstrated antibacterial activity, UV shielding, and real-food preservation performance, thereby offering both scientific novelty and application-oriented innovation to the field of food packaging. Looking ahead, future work should focus on mechanistic investigations such as surface characterization and microbial adhesion assays to provide deeper insights into how CBN contributes to antibacterial performance and to guide the rational design of next-generation active packaging films.

CRedit authorship contribution statement

Siti Hajar Othman: Writing – review & editing, Visualization, Validation, Supervision, Resources, Project administration, Funding acquisition, Data curation, Conceptualization. **Nur Syahira Zaid:** Writing – original draft, Validation, Methodology, Investigation, Formal analysis. **Ruzanna Ahmad Shapi'i:** Validation, Supervision. **Norhazirah Nordin:** Validation, Supervision. **Rosnita A. Talib:** Validation, Supervision. **Intan Syafinaz Mohamed Amin Tawakkal:** Validation, Supervision.

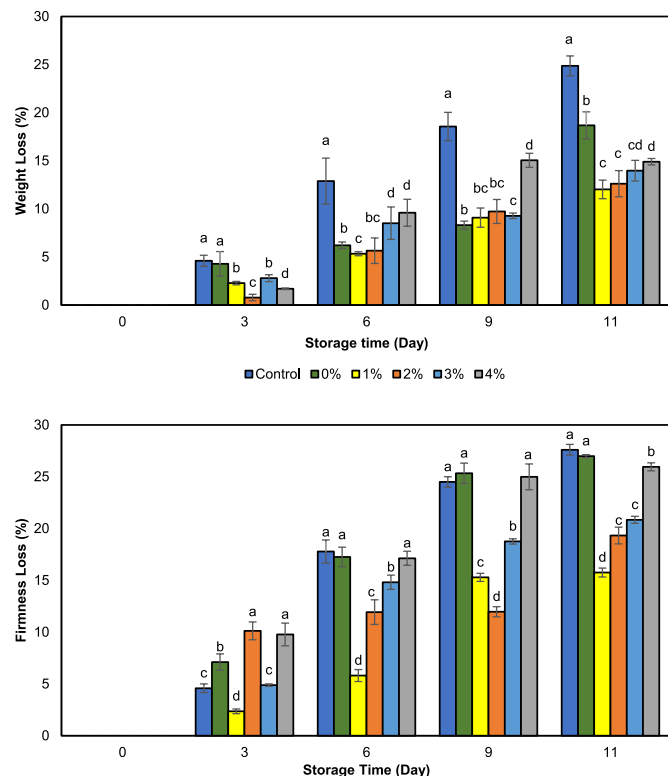


Fig. 7. (a) Percentage weight loss and (b) firmness loss of unpackaged and packaged cherry tomatoes with the neat starch and starch/CBN (1, 2, 3, 4 %w/v) films during 11 days storage at 10 °C. Different letters in the same storage day indicate a statistically significant difference ($p < 0.05$).

Declaration of competing interest

The authors declare that they have no known competing financial interests or personal relationships that could have appeared to influence the work reported in this paper.

Acknowledgments

This research was funded by the Ministry of Higher Education Malaysia, under the Fundamental Research Grant Scheme (FRGS/1/2024/TK05/UPM/02/9).

Data availability

The data that support the findings of this study are available from the corresponding authors upon reasonable request.

References

- [1] B. Freedman, W. Dorsey, A. Frazier, M. Kambhampati, J. Galiotos, S. Mukherjee, Chapter 5 ~ biodegradable and non-biodegradable waste. <https://louis.pressbooks.pub/environmentalscience/chapter/chapter-5/>, 2024. (Accessed 28 February 2025).
- [2] S.H. Othman, R.A. Shapi'i, N.D.A. Ronzi, Starch biopolymer films containing chitosan nanoparticles: a review, *Carbohydr. Polym.* 329 (2023) 121735, <https://doi.org/10.1016/j.carbpol.2023.121735>.
- [3] R.A. Shapi'i, S.H. Othman, R.K. Basha, M.N. Naim, Mechanical, thermal, and barrier properties of starch films incorporated with chitosan nanoparticles, *Nanotechnol. Rev.* 11 (2022) 1464–1477, <https://doi.org/10.1515/NTREV-2022-0094>.
- [4] C. Cui, N. Ji, Y. Wang, L. Xiong, Q. Sun, Bioactive and intelligent starch-based films: a review, *Trends Food Sci. Technol.* 116 (2021) 854–869, <https://doi.org/10.1016/j.tifs.2021.08.024>.
- [5] D. Yun, H. Cai, Y. Liu, L. Xiao, J. Song, J. Liu, Development of active and intelligent films based on cassava starch and Chinese bayberry anthocyanins (*Myrica rubra* Sieb. et Zucc.) anthocyanins, *RSC Adv.* 9 (2019) 30905–30916, <https://doi.org/10.1039/C9RA06628D>.
- [6] S.H. Othman, N.F.L. Othman, R.A. Shapi'i, S.H. Ariffin, K.F.M. Yunus, Corn starch/chitosan nanoparticles/thymol bio-nanocomposite films for potential food packaging applications, *Polymers* 13 (2021) 390, <https://doi.org/10.3390/polym13030390>.
- [7] M.A. Sani, A. Khezrelou, M. Rezvani-Ghalhari, D.J. McClements, R.S. Varma, Advanced carbon-based nanomaterials: application in the development of multifunctional next-generation food packaging materials, *Adv. Colloid Interface Sci.* 339 (2025) 103422, <https://doi.org/10.1016/j.cis.2025.103422>.
- [8] N.S. Kasálková, P. Slepíčka, V. Švorčík, I. Rodríguez-Ramos, M. Al-Haik, Carbon nanostructures, nanolayers, and their composites, *Nanomaterials* 11 (2021) 2368, <https://doi.org/10.3390/nano11092368>.
- [9] Z. Shi, L. Hua, Y. Lu, D. Shen, D. Huang, Investigation of carbon black nanoparticle modified cementitious composites for sensing dynamic vibro-acoustic signals, *Measurement* 237 (2024) 115231, <https://doi.org/10.1016/j.measurement.2024.115231>.
- [10] M.P. Ho, A.K.T. Lau, Amorphous carbon nanocomposites, in: Y. Dong, R. Umer, A. K.T. Lau (Eds.), *Fillers and Reinforcements for Advanced Nanocomposites*, Woodhead Publishing, Cambridge, 2015, pp. 309–328, <https://doi.org/10.1016/B978-0-08-100079-3.00012-0>.
- [11] A. Khoshkalampour, M. Ghorbani, Z. Ghasempour, Cross-linked gelatin film enriched with green carbon quantum dots for bioactive food packaging, *Food Chem.* 404 (2022) 134742, <https://doi.org/10.1016/j.foodchem.2022.134742>.
- [12] A. Khan, R. Priyadarshi, T. Bhattacharya, J. Rhim, Carrageenan/Alginate-based functional films incorporated with Allium sativum carbon dots for UV-barrier food packaging, *Food Bioprocess Technol.* 16 (2023) 2001–2015, <https://doi.org/10.1007/s11947-023-03048-7>.
- [13] S.M. Dizaj, A. Mennati, S. Jafari, K. Khezri, K. Adibkia, Antimicrobial activity of carbon-based nanoparticles, *Adv. Pharmaceut. Bull.* 5 (2015) 19–23, <https://doi.org/10.5681/APB.2015.003>.
- [14] O. Das, A.J. Capezza, J. Mårtensson, Y. Dong, R.E. Neisiany, L. Pelcastre, L. Jiang, Q. Xu, R.T. Olsson, M.S. Hedenqvist, The effect of carbon black on the properties of plasticised wheat gluten biopolymer, *Molecules* 25 (2020) 2279, <https://doi.org/10.3390/molecules25102279>.
- [15] ASTM D882, Standard test method for tensile properties of thin plastic sheeting. www.astm.org/d0882-18.html, 2018. (Accessed 28 February 2025).
- [16] JIS Z0208, Testing methods for determination of the water vapour transmission rate of moisture-proof packaging materials (dish method). <https://webstore.ansi.org/standards/jis/jis02081976>, 1976. (Accessed 16 June 2025).
- [17] ASTM D3985, Standard test method for oxygen gas transmission rate through plastic film and sheeting using a coulometric sensor. www.astm.org/d3985-17.html, 2024. (Accessed 28 February 2025).
- [18] USDA, United States standards for grades of fresh tomatoes. https://www.ams.usd.gov/sites/default/files/media/Tomato_Standard%5B1%5D.pdf, 1997. (Accessed 3 March 2025).
- [19] M.Ö. Alaş, G. Doğan, M.S. Yalcin, S. Ozdemir, R. Genç, Multicolor emitting carbon dot-reinforced PVA composites as edible food packaging films and coatings with antimicrobial and UV-blocking properties, *ACS Omega* 7 (2022) 29967–29983, <https://doi.org/10.1021/acsomega.2c02984>.
- [20] J.E. Lee, K. Chung, Y.H. Jang, Y.J. Jang, S.T. Kochuveedu, D. Li, D.H. Kim, Bimetallic multifunctional core@shell plasmonic nanoparticles for localized surface plasmon resonance based sensing and electrocatalysis, *Anal. Chem.* 84 (2012) 6494–6500, <https://doi.org/10.1021/ac300654k>.
- [21] R.R. Koshy, J.T. Koshy, S.K. Mary, S. Sadanandan, S. Jisha, L.A. Pothen, Preparation of pH sensitive film based on starch/carbon nano dots incorporating anthocyanin for monitoring spoilage of pork, *Food Control* 126 (2021) 108039, <https://doi.org/10.1016/j.foodcont.2021.108039>.
- [22] G. Fredi, M.K. Jafari, A. Dorigato, D.N. Bikiaris, A. Pegoretti, Improving the thermomechanical properties of poly(lactic acid) via reduced graphene oxide and bioderived poly(decamethylene 2,5-furandicarboxylate), *Mater* 15 (2022) 1316, <https://doi.org/10.3390/ma15041316>.
- [23] T. Albright, J. Hobeck, Characterization of carbon-black-based nanocomposite mixtures of varying dispersion for improving stochastic model fidelity, *Nanomaterials* 13 (2023) 916, <https://doi.org/10.3390/nano13050916>.
- [24] J. Ding, X. Wu, X. Qi, H. Guo, A. Liu, W. Wang, Impact of nano/micron vegetable carbon black on mechanical, barrier and anti-photooxidation properties of fish gelatin film, *J. Sci. Food Agric.* 98 (2018) 2623–2641, <https://doi.org/10.1002/jsfa.8756>.
- [25] C. Campalani, V. Causin, M. Selva, A. Perosa, Fish-waste-derived gelatin and carbon dots for biobased UV-blocking films, *ACS Appl. Mater. Interfaces* 14 (30) (2022) 35148–35156, <https://doi.org/10.1021/ACSAMI.2C11749>.
- [26] W.D. Callister, D.G. Rethwisch, *Materials Science and Engineering: an Introduction*, ninth ed., John Wiley & Sons, Inc., New Jersey, 2014.
- [27] K. Nare, S.P. Hlangothi, Thermorheological evaluation of antiaging behavior of four antioxidants in 70/100 bitumen, *J. Mater. Civ. Eng.* 31 (5) (2019) 04019034, [https://doi.org/10.1061/\(ASCE\)MT.1943-5533.0002658](https://doi.org/10.1061/(ASCE)MT.1943-5533.0002658).
- [28] R. Venkatesan, P. Sivaprakash, I. Kim, G.E. Eldesoky, S.C. Kim, Tannic acid as a crosslinking agent in poly(butylene adipate-co-terephthalate) composite films enhanced with carbon nanoparticles: processing, characterization, and antimicrobial activities for food packaging, *J. Environ. Chem. Eng.* 11 (4) (2023) 110194, <https://doi.org/10.1016/J.JECE.2023.110194>.
- [29] A. Sommereyns, T. Hupfeld, S. Gann, T. Wang, C. Wu, E. Zhuravlev, A. Lüddecke, S. Baumann, J. Rudloff, M. Lang, B. Göke, S. Barcikowski, M. Schmidt, Influence of sub-monolayer quantities of carbon nanoparticles on the melting and crystallization behavior of polyamide 12 powders for additive manufacturing, *Mater. Des.* 201 (2021) 109487, <https://doi.org/10.1016/j.matdes.2021.109487>.
- [30] M. Mousa, Y. Dong, I.J. Davies, Eco-friendly polyvinyl alcohol (PVA)/bamboo charcoal (BC) nanocomposites with superior mechanical and thermal properties, *Adv. Compos. Mater.* 27 (5) (2016) 499–509, <https://doi.org/10.1080/09243046.2017.1407906>.
- [31] J.-W. Rhim, P.K.W. Ng, Natural biopolymer-based nanocomposite films for packaging applications, *Crit. Rev. Food Sci. Nutr.* 47 (2007) 411–433, <https://doi.org/10.1080/10408390600846366>.
- [32] M.P. Arrieta, E. Fortunati, F. Dominici, E. Rayón, J. López, J.M. Kenny, Multifunctional PLA-PHB/cellulose nanocrystal films: processing, structural and thermal properties, *Carbohydr. Polym.* 121 (2015) 265–275, <https://doi.org/10.1016/j.carbpol.2014.12.060>.
- [33] V. Siracusa, P. Rocculi, S. Romani, M.D. Rosa, Biodegradable polymers for food packaging: a review, *Trends Food Sci. Technol.* 19 (2008) 634–643, <https://doi.org/10.1016/j.tifs.2008.07.003>.
- [34] A. Sorrentino, G. Gorrasi, V. Vittoria, Potential perspectives of bio-nanocomposites for food packaging applications, *Trends Food Sci. Technol.* 18 (2007) 84–95, <https://doi.org/10.1016/j.tifs.2006.09.004>.
- [35] H.M.C. Azeredo, Nanocomposites for food packaging applications, *Food Res. Int.* 42 (2009) 1240–1253, <https://doi.org/10.1016/j.foodres.2009.03.019>.
- [36] A. Kwaśniewska, M. Świetlicki, A. Prószyński, G. Gładyszewski, Physical properties of starch/powdered activated carbon composite films, *Polymers* 13 (24) (2021) 4406, <https://doi.org/10.3390/POLYM13244406>.
- [37] J. Jin, R. Rafiq, Y.Q. Gill, M. Song, Preparation and characterization of high performance of graphene/nylon nanocomposites, *Eur. Polym. J.* 49 (9) (2013) 2617–2626, <https://doi.org/10.1016/J.EURPOLYMJ.2013.06.004>.
- [38] B. Alexandre, D. Langevin, P. Médéric, T. Aubry, H. Couderc, Q.T. Nguyen, A. Saiter, S. Marais, Water barrier properties of polyamide 12/montmorillonite nanocomposite membranes: structure and volume fraction effects, *J. Membr. Sci.* 328 (1–2) (2009) 186–204, <https://doi.org/10.1016/J.MEMSCI.2008.12.004>.
- [39] R. Shogren, Water vapor permeability of biodegradable polymers, *J. Environ. Polym. Degrad.* 5 (1997) 91–95, <https://doi.org/10.1007/bf02763592>.
- [40] Polymer Synthese Werk GmbH, What is the water vapor permeability of PE?. https://www.polymersynthese.com/en/home/faqs/water-vapor-permeability?utm_source. (Accessed 21 August 2025).
- [41] Packaging Flair, What is oxygen transmission rate (OTR)?. <https://www.flairpackaging.com/post/what-is-oxygen-transmission-rate-otr?>. (Accessed 21 August 2025).
- [42] M. Sharif Sh, F. Golestani Fard, E. Khatibi, H. Sarpoolaky, Dispersion and stability of carbon black nanoparticles, studied by ultraviolet–visible spectroscopy, *J. Taiwan Inst. Chem. Eng.* 40 (5) (2009) 524–527, <https://doi.org/10.1016/J.JTICE.2009.03.006>.
- [43] J. Pouch, S. Alterovitz, Properties and Characterization of Amorphous Carbon Films, *Trans Tech Publ.*, Switzerland, 1990, <https://doi.org/10.4028/b-y46rb4>.

- [44] P. Uthirakumar, M. Devendiran, T.H. Kim, I.H. Lee, A convenient method for isolating carbon quantum dots in high yield as an alternative to the dialysis process and the fabrication of a full-band UV blocking polymer film, *New J. Chem.* 42 (22) (2018) 18312–18317, <https://doi.org/10.1039/C8NJ04615H>.
- [45] M. Darré, A.R. Vicente, L. Cisneros-Zevallos, F. Artés-Hernández, Postharvest ultraviolet radiation in fruit and vegetables: applications and factors modulating its efficacy on bioactive compounds and microbial growth, *Foods* 11 (5) (2022) 653, <https://doi.org/10.3390/FOODS11050653>.
- [46] G. Kavoosi, S.M.M. Dadfar, S.M.A. Dadfar, F. Ahmadi, M. Niakosari, Investigation of gelatin/multi-walled carbon nanotube nanocomposite films as packaging materials, *Food Sci. Nutr.* 2 (1) (2014) 65–73, <https://doi.org/10.1002/FSN3.81>.
- [47] S.F. Hosseini, M. Rezaei, M. Zandi, F. Farahmandghavi, Fabrication of bio-nanocomposite films based on fish gelatin reinforced with chitosan nanoparticles, *Food Hydrocoll.* 44 (2015) 172–182, <https://doi.org/10.1016/J.FOODHYD.2014.09.004>.
- [48] M. Ahmad, S. Benjakul, T. Prodpran, T.W. Agustini, Physico-mechanical and antimicrobial properties of gelatin film from the skin of unicorn leatherjacket incorporated with essential oils, *Food Hydrocoll.* 28 (1) (2012) 189–199, <https://doi.org/10.1016/J.FOODHYD.2011.12.003>.
- [49] K. Mitura, J. Kornacka, E. Kopczyńska, J. Kalisz, E. Czerwińska, M. Affeltowicz, W. Kaczorowski, B. Kolesińska, J. Frączyk, T. Bakalova, L. Svobodová, P. Louda, Active carbon-based nanomaterials in food packaging, *Coatings* 11 (2) (2021) 161, <https://doi.org/10.3390/coatings11020161>.
- [50] K. Fan, M. Zhang, D. Fan, F. Jiang, Effect of carbon dots with chitosan coating on microorganisms and storage quality of modified-atmosphere-packaged fresh-cut cucumber, *J. Sci. Food Agric.* 99 (13) (2019) 6032–6041, <https://doi.org/10.1002/JSFA.9879>.
- [51] P. Li, L. Sun, S. Xue, D. Qu, L. An, X. Wang, Z. Sun, Recent advances of carbon dots as new antimicrobial agents, *SmartMat* 3 (2) (2022) 226–248, <https://doi.org/10.1002/SMM2.1131>.
- [52] H. Li, J. Huang, Y. Song, M. Zhang, H. Wang, F. Lu, H. Huang, Y. Liu, X. Dai, Z. Gu, Z. Yang, R. Zhou, Z. Kang, Degradable carbon dots with broad-spectrum antibacterial activity, *ACS Appl. Mater. Interfaces* 10 (32) (2018) 26936–26946, <https://doi.org/10.1021/ACSAMI.8B08832>.
- [53] N. Saba, M.T. Paridah, M. Jawaid, M. Asim, Carbon nanomaterials as antimicrobial agents to combat multidrug resistance, in: M.Y. Wani, I.A. Wani, A. Rai (Eds.), *Nanomaterials for Sustainable Energy and Environmental Remediation*, Springer, Singapore, 2024, pp. 215–240. https://link.springer.com/chapter/10.1007/978-981-97-2023-1_9.
- [54] S. Kang, M. Pinault, L.D. Pfefferle, M. Elimelech, Antibacterial effects of carbon nanotubes: size does matter, *Langmuir* 24 (2008) 6409–6413, <https://doi.org/10.1021/la800951v>.
- [55] O. Akhavan, E. Ghaderi, Toxicity of graphene and graphene oxide nanowalls against bacteria, *ACS Nano* 4 (2010) 5731–5736, <https://doi.org/10.1021/nn101390x>.
- [56] X. Liu, J. Wang, Z. Feng, L. Zhang, B. Yang, Antibacterial activity of graphite, graphite oxide, graphene oxide, and reduced graphene oxide: membrane and oxidative stress, *ACS Nano* 5 (2011) 6971–6980, <https://doi.org/10.1021/nn202451x>.
- [57] V. Paul, R. Pandey, Role of internal atmosphere on fruit ripening and storability—a review, *J. Food Sci. Technol.* 51 (7) (2011) 1223–1250, <https://doi.org/10.1007/s13197-011-0583-x>.
- [58] T.T. Pham, L.L.P. Nguyen, M.S. Dam, L. Baranyai, Application of edible coating in extension of fruit shelf life: review, *AgriEngineering* 5 (1) (2023) 520–536, <https://doi.org/10.3390/agriengineering5010034>.
- [59] M. Linke, M. Geyer, Condensation dynamics in plastic film packaging of fruit and vegetables, *J. Food Eng.* 116 (1) (2012) 144–154, <https://doi.org/10.1016/j.jfoodeng.2012.11.026>.
- [60] R.S. Matche, Packaging aspects of fruits and vegetables, in: G.C.P. Rangarao (Ed.), *Plastics in Food Packaging*, Indian Centre for Plastics in the Environment, Mumbai, 2023, pp. 115–132. <https://www.icpe.in/Plastics%20in%20Food%20Packaging/pdf/6-Final.pmd.pdf>.
- [61] A. Conte, L. Angiolillo, M. Mastromatteo, M.A. Del Nobile, Technological options of packaging to control food quality, in: I. Muzzalupo (Ed.), *Food Industry*, IntechOpen, London, 2013, pp. 355–379, <https://doi.org/10.5772/53151>.
- [62] H. San, Y. Laurenza, E. Behzadfar, U. Sonchaeng, K. Wadaugsorn, J. Sodsai, T. Kaewpetch, K. Promhuad, A. Srira, P. Wongphan, N. Harnkarnsujarit, Functional polymer and packaging technology for bakery products, *Polymers* 14 (18) (2022) 3793, <https://doi.org/10.3390/polym14183793>.
- [63] E. Medina, N. Caro, L. Abugoch, A. Gamboa, M. Díaz-Dosque, C. Tapia, Chitosan thymol nanoparticles improve the antimicrobial effect and the water vapour barrier of chitosan-quinoa protein films, *J. Food Eng.* 240 (2019) 191–198, <https://doi.org/10.1016/J.JFOODENG.2018.07.023>.
- [64] P.B. Pathare, M. Al-Dairi, Effect of mechanical damage on the quality characteristics of banana fruits during short-term storage, *Discov. Food* 2 (1) (2022) 4, <https://doi.org/10.1007/s44187-022-00007-7>.
- [65] J. Wang, C. Shi, D. Fang, J. Che, W. Wu, L. Lyu, W. Li, The impact of storage temperature on the development of microbial communities on the surface of blueberry fruit, *Foods* 12 (8) (2023) 1611, <https://doi.org/10.3390/FOODS12081611>.